

A Deep Cavitand Receptor Functionalized with Fe(II) and Mn(II) Aminopyridine Complexes for Bioinspired Oxidation Catalysis.

Diego Vidal, Miquel Costas, and Agustí Lledó**

Institute of Computational Chemistry and Catalysis, and Department of Chemistry, Universitat de Girona, c/Maria Aurèlia de Capmany 69, 17003 Girona, Spain.

ABSTRACT: A deep cavitand receptor **2** based on a resorcinarene scaffold and functionalized with a bis(pyridyl)dipyrrolidine tetradentate ligand has been obtained. Binding of divalent metal ions ($M^{2+} = Mn^{2+}$, Fe^{2+} and Zn^{2+}) at the tetradentate ligand results in the formation of cavitand complexes $2 \cdot M(OTf)_2$. The complexes exhibit selective binding of alkylammonium ions and amides within the cavitand. $2 \cdot M(OTf)_2$ ($M = Fe(II)$ and $Mn(II)$) catalyze selective hydroxylation of aliphatic C–H bonds and epoxidation of olefins with hydrogen peroxide, exhibiting selectivity patterns consistent with the implication of high valent metal-oxo species. Furthermore, $2 \cdot Fe(OTf)_2$ reacts with IO_4^- to form an oxoiron(IV) complex $[2 \cdot Fe(O)]^{2+}$, without decomposition of the supramolecular container. This species is relatively stable at 0 °C, yet engages in fast oxygen atom transfer reactions.

KEYWORDS: supramolecular chemistry, cavitands, bioinspired catalysis, oxidation catalysis, non-heme metal complexes, high valent oxo species.

INTRODUCTION

The mimicry of enzymatic catalysis with artificial systems has been a long standing goal of synthetic supramolecular chemistry.¹ It is now widely accepted that, in order to rival the proficiency of enzymes, an artificial system must be built so that it defines a confined space where the substrate is isolated from bulk medium and exposed to direct contact with appropriate functional groups, a distinct feature of proteins and enzymes. The large and diverse family of metal-dependent oxidation enzymes provides remarkable examples of such specialized microenvironments, in which highly reactive transition metal centers are contained and kept from reacting with the protein backbone, while effecting selective oxidations of complementary substrates.²

Significant advances in the mimicry of enzymatic oxidations have been made employing carefully designed synthetic coordination compounds of assorted transition metals.³ Among these, non-heme Fe and Mn complexes bearing tetradentate nitrogen chelating ligands stand out because of their oxidation prowess.⁴ Such complexes are appealing from the synthetic point of view: they are efficient oxidants of C–H and C=C bonds –even at low catalyst loadings– employing green oxidants such as hydrogen peroxide, they can perform asymmetric reactions, and they are based on abundant first row transition metals. Overall, these catalysts represent a green and sustainable option for oxidative transformations of organic compounds. However, the incorporation of the aforementioned Fe and Mn coordination manifolds into a supramolecular scaffold with a confined space suitable for substrate binding remains virtually unexplored.⁵ This approximation has the potential to unveil new reactivity patterns, and even to override the innate

selectivity of a substrate when multiple C–H or C=C bonds are present. We present herein our first take on this approach, combining a self-folding deep cavitand receptor⁶ with a bis(pyridyl)dipyrrolidine (pdp) chelator suitable for Fe and Mn catalyzed oxidation chemistry (Fig. 1).⁷

RESULTS AND DISCUSSION

Resorcinarene-based self-folding cavitands (**1**, Fig. 1) are capable of binding small hydrophobic molecules and organic cations whose exchange process is regulated by a seam of hydrogen bonded secondary amides akin to that defining secondary structure in proteins. More importantly, desymmetrized versions are accessible which allow the incorporation of inwardly directed functional groups, allowing the stabilization of elusive reactive intermediates⁸ and enabling biomimetic organocatalysis.⁹ Several metal containing receptors have also been prepared with this approach.^{7,10,11} For our receptor **2** (Fig. 1), we decided to use an acetal bridge as the attaching point¹² for the ligand –rather than the more customary benzimidazole moiety–,^{7,10a-e} with the aim of bringing the metal reactive center as close as possible to the deep section of the cavity. Preliminary modelling studies suggested that a *meta* substituted pyridine would provide a relatively unhindered metal coordination site on the side of the cavity. Bearing in mind the importance of ligand effects on Fe/Mn oxidation chemistry,⁴ we sought to develop a synthetic plan amenable to modification and diversification at a late stage. Unlike other iron-containing supramolecular constructs, our design combines a sizable molecular recognition motif with a structured and well-defined coordination environment.¹³

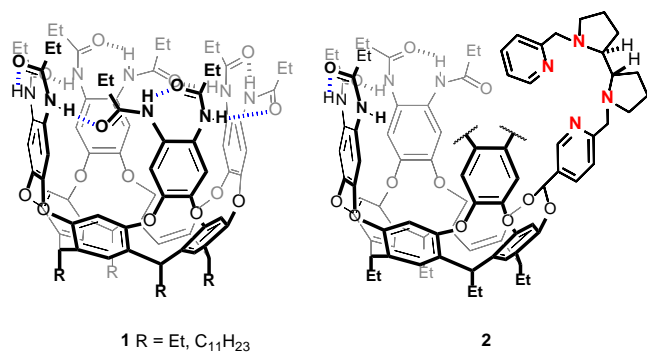
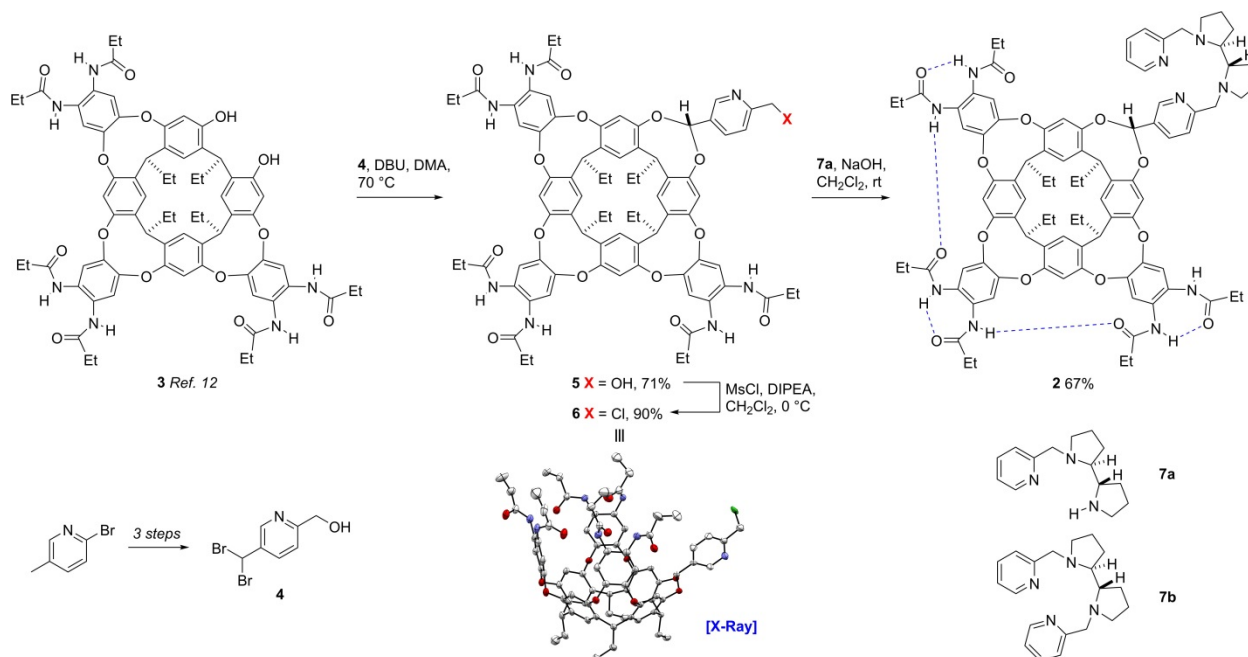


Figure 1. The parent octa(amido) self-folding cavitand **1** and its bis(pyridyl)dipyrrolidine-functionalized derivative **2** (some fragments omitted for clarity).

The synthesis of **2** started from the versatile hexaamido-diol cavitand **3** (Scheme 1).¹⁴ After some experimentation, we found that condensation of **3** with meta substituted dibromomethyl pyridine **4** proceeded cleanly and in good yield.¹⁵ Pyridine building block **4** was prepared in **3** steps from commercially available 2-bromo-5-methylpyridine (see SI). Mesylation of hydroxyl derivative **5** with mesyl chloride proceeded with concomitant substitution by chloride to deliver key intermediate **6**, which was univocally characterized by X-ray crystallography. Nucleophilic displacement of 2-chloromethylpyridine derivative **6** with secondary amines appears as an attractive entry into structurally diverse cavitand-ligand hybrids. For the work presented herein we chose to use known pyridyl bispyrrolidine (*S,S*)-**7a**,¹⁶ which reacted smoothly with **6** in the presence of base to deliver cavitand **2** in good yield. Cavitand **2** was characterized by ¹H and ¹³C NMR, HRMS and EA (see SI).

Scheme 1. Synthesis of cavitant **2** (only one of the interconverting cyclodiastereomers is depicted).



The directionality established on of the hydrogen bond seam formed by the amide groups renders cavitant **1** chiral. In the absence of hydrogen bond disrupting molecules, **1** exists as an even mixture of two *cycloenantiomers* which interconvert slowly relative to the NMR time scale.⁶ Accordingly, **2** must exist –by virtue of the added homochiral ligand fraction– as an undetermined mixture of *cyclodiastereomers*. These may appear as different sets of signals in the ¹H NMR spectrum, complicating further analysis. However, in the presence of acetone-*d*₆ amide rotation is fast in the NMR time scale, notably simplifying the ¹H NMR spectrum (Fig. 2). Because of its distance to the chiral backbone of the ligand, the amide NH's experience little magnetic asymmetry, and therefore appear as three separate resonances only.

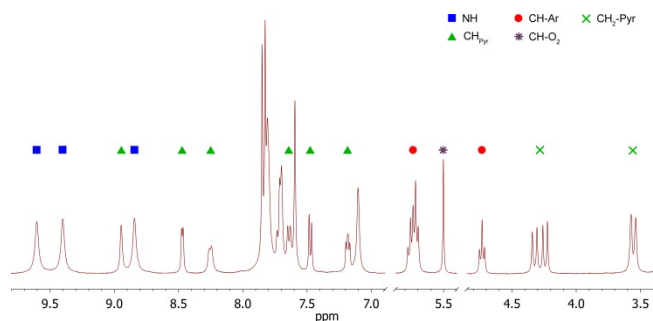
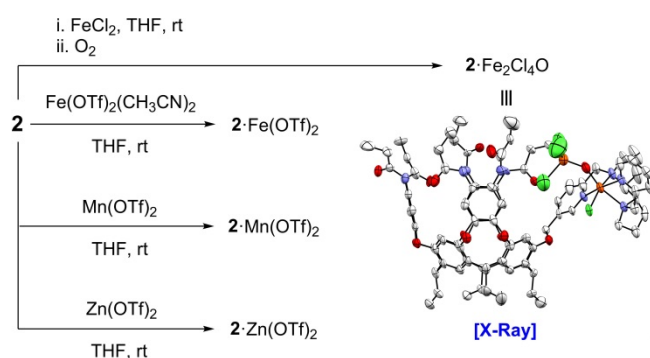


Figure 2. Selected regions and assignment of the ^1H NMR spectrum of **2** (400 MHz, acetone- d_6).

With cavitand **2** in hand, we then proceeded to explore its coordination chemistry with different transition metals (Scheme 2). Upon reaction with Fe(II), Mn(II) or Zn(II) triflate salts in THF, the corresponding cavitand complexes were obtained cleanly as crystalline materials. The formation of the corresponding Fe and Mn complexes can be followed by UV-Vis spectroscopy, and in the case of the Zn complex by ^1H -NMR spectroscopy. For the three cases, titration experiments confirm that each cavitand only binds one metallic center (see the SI). Interestingly, the Fe complex displays only subtle paramagnetic effects in its ^1H NMR spectra at 300K, indicating that the ferrous center is in the diamagnetic low spin state. This is in sharp contrast to the parent $[\text{Fe}(\text{pdp})(\text{CH}_3\text{CN})_2]^{2+}$ family of complexes, that possess high spin ferrous centers,¹⁷ suggesting a subtle influence of the cavitand in modulating the electronic properties of the metal center. We also prepared the analogous Zn complex as a surrogate devoid of paramagnetic interferences, in order to better study the host-guest properties of our system by ^1H NMR. In addition to triflate ligated compounds with potential for catalysis (*vide infra*), we obtained an Fe dimer coordinated analogue by treatment of **2** with FeCl_2 and subsequent exposure to air. Crystals of $\mathbf{2}\cdot\text{Fe}_2\text{Cl}_3\text{O}$ suitable for X-ray diffraction were obtained, which revealed the desired coordination arrangement through the tetradentate ligand facing the cavity of the receptor

(Scheme 2). Importantly, this layout does not interfere with binding of small molecules in the cavity (occupied by solvent in the structure obtained).

Scheme 2. Complex synthesis and X-ray diffraction structure of $2 \cdot \text{Fe}_2\text{Cl}_4\text{O}$ (gray: C, blue: N, red: O, green: Cl, orange: Fe; solvent molecules omitted for clarity).



Next, we proceeded to evaluate the host-guest properties of cavitand **2** and its metal complexes. We chose to use acetonitrile as a solvent preferentially, since it is the most suitable for Fe- or Mn- catalyzed oxidations.⁴ Resorcinarene-based deep cavitands typically abhor polar solvents such as methanol or acetonitrile, forcing the adoption of a flat *kite* conformation which dimerizes through π - π stacking interactions.¹⁸ In our case, however, the methine resonances at $\delta \sim 5.6$ ppm in the ^1H NMR spectrum of **2** and its metal complexes in CD_3CN reveal a folded vase conformation in each case (see the SI). The addition of the nitrogenated ligand or its cationic complexes renders the cavity less hydrophobic and allows the accommodation of more polar guests, as seen in the X-ray structures obtained. Neutral guests with well-established complementarity for **1**, such as 1-adamantanecarbonitrile (**8a**, Fig. 3),¹⁹ do not displace the solvent molecules in the cavity to provide kinetically stable complexes with $2 \cdot \text{M(OTf)}_2$. The addition of a cationic anchor enables the formation of kinetically stable complexes, diagnosed by the occurrence of resonances in the far upfield region of the spectrum (δ 0 to -4 ppm),

corresponding to buried aliphatic protons (Figure 3).²⁰ The large upfield shifts observed are consistent with the receptor retaining the vase conformation,²¹ and the chemical shifts of the methine protons in the resulting host-guest complexes corroborate this hypothesis (see SI). Guests **8b-c**, **9** and **10** bind with their bulky aliphatic portions buried deep in the aromatic cavity through CH- π interactions, leaving the ammonium group within suitable range to establish additional interactions with the amide groups. For primary and secondary ammonium moieties hydrogen bonding to the amide's carbonyls is established, whereas quaternary ammonium groups establish cation-dipole interactions when the charged portion is positioned near the rim, as is the case with **9**.²² In the absence of such secondary interactions, a guests cannot compete with the solvent which is present in large excess. Interestingly, ambidextrous guest **8c** binds with the smaller cyclohexyl moiety positioned in the cavity as ascertained by 2D NMR (see SI), suggesting a slightly reduced binding space in the metallo-cavitands with respect to **1**. Finally, cyclohexylamine amides (**11**) are also good guests, thanks to the occurrence of hydrogen bonding interactions with the other amide groups on the rim of the cavity.

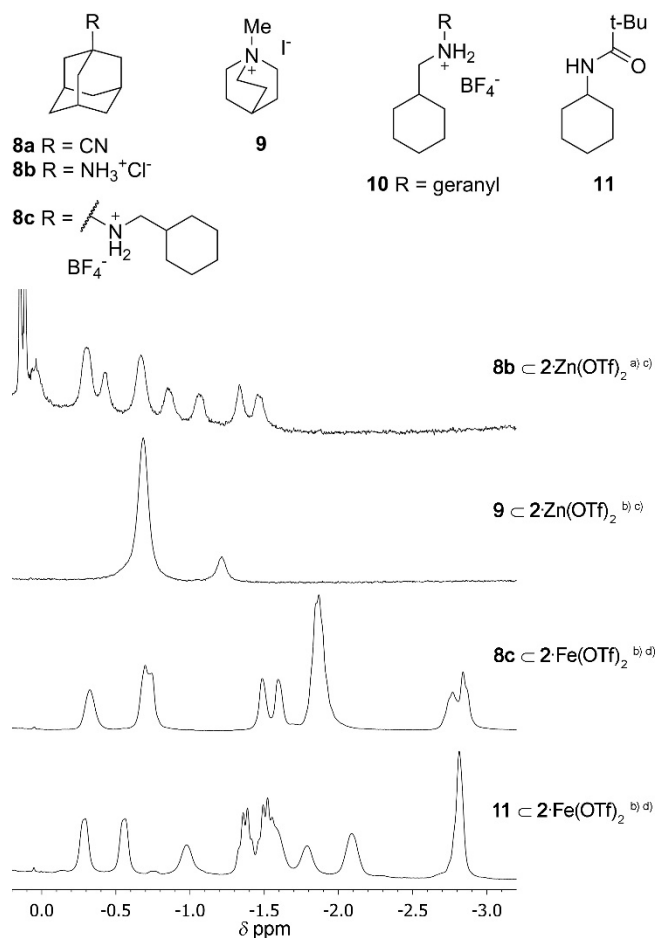
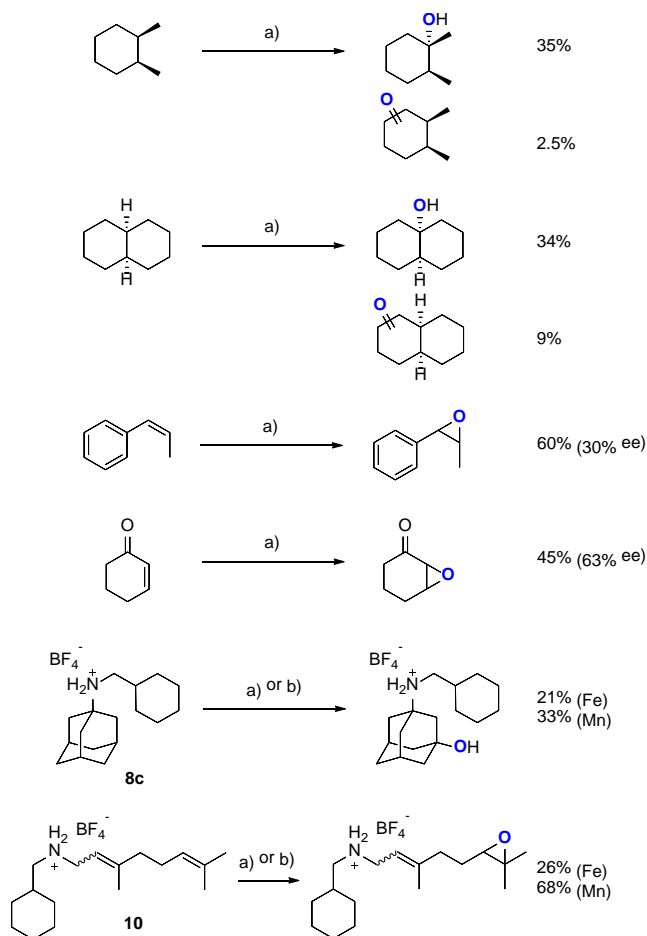


Figure 3. Guests used in this study and upfield regions in the ¹H NMR spectra of complexes with **2**·M(OTf)₂. a) In acetone-*d*₆. b) in CD₃CN. c) at 298 K. d) at 240 K.

We then proceeded to evaluate complexes **2**·Fe(OTf)₂ in representative iron catalyzed C–H and C=C bond oxidations using hydrogen peroxide as terminal oxidant (Scheme 3). Most notably, **2**·Fe(OTf)₂ presents sustained catalytic activity in C–H hydroxylation and olefin epoxidation reactions. Monitoring of the iron species by ESI-MS during catalysis reveals that the integrity of the complex is retained during the time course of the reaction. Under non-optimized reaction conditions, hydroxylation of *cis*-1,2-dimethylcyclohexane and *cis*-decalin occurs selectively at the tertiary C–H bond, is stereospecific and the corresponding tertiary alcohol is obtained in 34–35% yield. Minor amounts of products (3–9%) resulting from methylene

oxidation are also obtained. Catalytic epoxidation of *cis*- β -methyl styrene and 2-cyclohexenone are also accomplished, producing the corresponding epoxides with absolute retention of configuration in 60% and 45% respective yields, and notable levels of enantioselectivity (30 and 63% ee respectively). The stereoretentive and stereoselective nature of the reactions constitute strong evidence that the reactions are mediated by selective metal based oxidants, most likely a highly electrophilic high valent metal-oxo ($M^V=O$, M = Fe or Mn) species.⁴ For the substrates so far mentioned we did not find evidence for the formation of *kinetically stable* host-guest complexes with $2 \cdot M(OTf)_2$, despite being appropriate in size.

Scheme 3. Catalytic oxidations with Fe and Mn catalysts. a) **2**·Fe(OTf)₂ (3 mol %), H₂O₂ (2.5 eq.), AcOH (1.5 eq.), MeCN, 0 °C, 30 min. b) **2**·Mn(OTf)₂ (1 mol %), H₂O₂ (2.0 eq.), AcOH (17 eq.), MeCN, 0 °C, 30 min.



Oxidation of **8c** and **10**, substrates that do form kinetically stable complexes with the cavitand, also takes place. Oxidation of **8c** occurs selectively at a tertiary C–H bond of the adamantane core, while epoxidation of **10** occurs at the most remote olefinic site from the ammonium unit. In both cases, the manganese catalyst exhibits a better performance than the iron analog. Unfortunately, the selectivity pattern observed in these cases is the same as the one observed with the parent [M(OTf)₂(pdp)] (**7b**·M(OTf)₂, M = Fe and Mn) catalysts. This suggests that the selectivity in these reactions is governed by the innate reactivity of the substrate, and that

substrate recognition does not have an impact on site selectivity. A supramolecular effect could potentially favor, for example, oxidation of a secondary C–H bond close in space to the metal center over a tertiary one which is away from it. Alternatively, it is also possible that oxidation occurs at substrate molecules when they are not bound to the cavitand.²³ The combination of these results thus evidences a powerful catalytic activity of the supramolecular catalysts, but also limitations in our design that will be addressed in future catalyst generations. Presumably, low barrier rotation of the pyridyl-acetal linkage orientates the metal active oxidant towards the outside of the cavity, preventing synergistic binding and oxidation of the substrate.

We finally assessed the ability of **2**·Fe(OTf)₂ to support the formation of high valent iron-oxo species of relevance to non-heme iron oxygenases.²⁴ Non-heme oxoiron (IV) complexes are highly reactive species which readily engage in C–H oxidation and oxygen transfer reactions.²⁵⁻²⁶ They are however, more stable than the oxoiron(V) species involved in catalytic C–H and C=C oxidations with H₂O₂/AcOH,⁴ and have been prepared and studied extensively employing simple coordination complexes.²⁵⁻²⁶ Nevertheless, their high reactivity is usually non compatible with elaborated supramolecular scaffolds, which would provide a chemically richer and closer model to enzymatic sites. Reaction of **2**·Fe(OTf)₂ with tetra(n-butyl)ammonium periodate (TBAPI, 1.2 equiv., TfOH 1.5 equiv.) was monitored by UV-Vis, revealing that the ferrous complex is smoothly converted to a new species [**2**·Fe(O)]²⁺ that exhibits a characteristic low energy band ($\lambda = 747 \text{ nm}$, $\epsilon = 210 \text{ M}^{-1} \text{ cm}^{-1}$) of a low spin ($S = 1$) iron (IV) oxo species (Fig. 4).²⁶ Indeed, ESI-MS analysis of the complex shows cluster ions at m/z 826.8238 and 1828.5134, consistent with [**2**·Fe^{IV}(O)]²⁺ and {[**2**·Fe^{IV}(O)](IO₃)}⁺ cations respectively. The spectrum also shows a peak at $m/z = 817.8180$ corresponding to an oxidative degradation entailing a formal desaturation reaction ([**2**·Fe^{II}-2H]²⁺). Peaks corresponding to analogous species are observed when

7b·Fe(OTf)₂ is reacted with TBAPI under analogous reaction conditions suggesting that formation of these species does not occur via oxidation of the cavitand. Remarkably, the new compound [2·Fe(O)]²⁺ remains relatively stable at 0 °C (t_{1/2} ~ 20 min), but it reacts rapidly (within seconds) with excess thioanisole,²⁷ producing 0.9 equiv. of the sulfoxide and regenerating 2·Fe(OTf)₂ (as shown by UV-Vis spectroscopy, see SI). Overall, this data indicates that the embedment of the complex in the cavitand stands the formation of high valent iron-oxo species without apparent degradation of the supramolecular vessel,²⁸ while not compromising its reactivity in oxygen atom transfer reactions against external substrates.

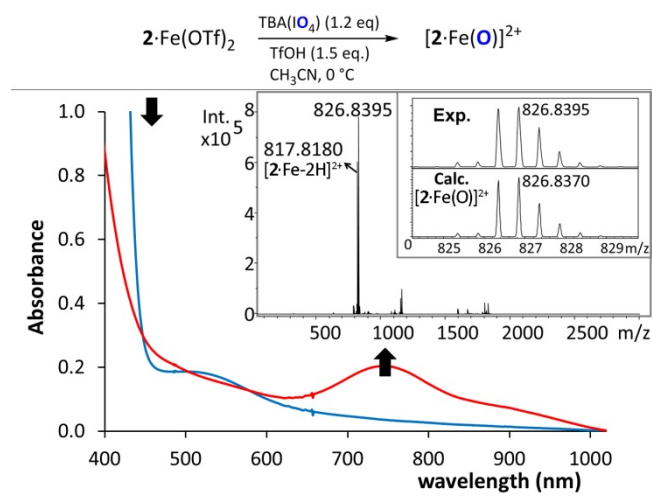


Figure 4. Formation of an Fe(IV) oxo species [2·Fe(O)]²⁺. Evolution of the UV-Vis spectra upon treatment of 2·Fe(OTf)₂ with TBAPI at 0 °C. Inset: ESI-MS spectrum of the same reaction mixture.

CONCLUSIONS

We have developed a new deep cavitand receptor functionalized with a chiral bis(pyridyl)dipyrrolidine ligand directed to metal coordination. The resulting Mn and Fe triflate derivatives are competent catalysts for the oxidation of CH and C=C bonds with hydrogen peroxide under mild conditions. The selectivities obtained in the oxidation reactions so far tested

with substrates that form kinetically stable complexes with the receptor do not significantly differ from those obtained with a model compound, suggesting that the oxidation steps are occurring to a significant extent outside the cavity. To the best of our knowledge, this system represents the first example of a sizeable container functionalized with a coordination complex capable of a) maintaining catalytic activity in selective C–H/C=C oxidation reactions,⁷ and b) supporting high valent metal-oxo species typically associated with such transformations.²⁸ Future developments in this area will address the limitations of the system presented, including the development of conformationally restricted analogues which prevented free rotation of the ligand scaffold. Our synthetic approach holds promise in this regard, since key intermediate **6** could be derivatized with a number of readily accessible and well established building blocks for the construction of tetradentate nitrogen ligands oriented towards early transition metal oxidation catalysis.⁴

ASSOCIATED CONTENT

Supporting Information.

Synthetic procedures and characterization data for new compounds. Detailed procedure for catalytic oxidation reactions. Formation and reactivity of Fe(IV) oxo species. Host-guest studies. 1D and 2D NMR, HRMS, UV-Vis spectra. X-ray diffraction data for **6** and **2**·Fe₂Cl₄O.

AUTHOR INFORMATION

Corresponding Author

* E-mail: agusti.lledo@udg.edu, miquel.costas@udg.edu

ACKNOWLEDGMENT

We thank MINECO - Spanish Government (“Ramón y Cajal” grant RYC2012-11112 and CTQ2014-54306-P to A.L., CTQ2015-70795-P to M.C.), Generalitat de Catalunya, (2014SGR931 and 2014SGR862), and Universitat de Girona (MPCUdG2016/096) for financial support.

REFERENCES

- (1) (a) Raynal, M.; Ballester, P.; Vidal-Ferran, A.; van Leeuwen, P. W. N. M., Supramolecular Catalysis. Part 2: Artificial Enzyme Mimics. *Chem. Soc. Rev.* **2014**, *43*, 1734-1787. (b) Meeuwissen, J.; Reek, J. N. H., Supramolecular Catalysis Beyond Enzyme Mimics. *Nat. Chem.* **2010**, *2*, 615-621.
- (2) (a) Solomon, E. I.; Heppner, D. E.; Johnston, E. M.; Ginsbach, J. W.; Cirera, J.; Qayyum, M.; Kieber-Emmons, M. T.; Kjaergaard, C. H.; Hadt, R. G.; Tian, L., Copper Active Sites in Biology. *Chem. Rev.* **2014**, *114*, 3659-3853. (b) Ortiz de Montellano, P. R., Hydrocarbon Hydroxylation by Cytochrome P450 Enzymes. *Chem. Rev.* **2010**, *110*, 932-948. (c) Kovaleva, E. G.; Lipscomb, J. D., Versatility of Biological Non-Heme Fe(II) Centers in Oxygen Activation Reactions. *Nat. Chem. Biol.* **2008**, *4*, 186-193.
- (3) Que, L.; Tolman, W. B., Biologically Inspired Oxidation Catalysis. *Nature* **2008**, *455*, 333-340.
- (4) (a) Olivo, G.; Cussó, O.; Borrell, M.; Costas, M., Oxidation of Alkane and Alkene Moieties with Biologically Inspired Nonheme Iron Catalysts and Hydrogen Peroxide: from Free Radicals to Stereoselective Transformations. *J. Biol. Inorg. Chem.* **2017**, *22*, 425-452. (b) Oloo, W. N.; Que, L., Bioinspired Nonheme Iron Catalysts for C–H and C=C Bond Oxidation: Insights into the Nature of the Metal-Based Oxidants. *Acc. Chem. Res.* **2015**, *48*, 2612-2621. (c) Bryliakov, K.

P.; Talsi, E. P., Active Sites and Mechanisms of Bioinspired Oxidation with H₂O₂, Catalyzed by Non-Heme Fe and Related Mn Complexes. *Coord. Chem. Rev.* **2014**, *276*, 73-96. (d) White, M. C., Adding Aliphatic C–H Bond Oxidations to Synthesis. *Science* **2012**, *335*, 807-809.

(5) Natarajan, N.; Brenner, E.; Sémeril, D.; Matt, D.; Harrowfield, J., The Use of Resorcinarene Cavitands in Metal-Based Catalysis. *Eur. J. Org. Chem.* **2017**, *2017*, 6100-6113.

(6) (a) Rudkevich, D. M.; Hilmersson, G.; Rebek, J., Self-Folding Cavitands. *J. Am. Chem. Soc.* **1998**, *120*, 12216-12225. (b) Rudkevich, D. M.; Hilmersson, G.; Rebek, J., Intramolecular Hydrogen Bonding Controls the Exchange Rates of Guests in a Cavitand. *J. Am. Chem. Soc.* **1997**, *119*, 9911-9912.

(7) Korom, S.; Ballester, P., Attachment of a RuII Complex to a Self-Folding Hexaamide Deep Cavitand. *J. Am. Chem. Soc.* **2017**, *139*, 12109-12112.

(8) Galan, A.; Ballester, P., Stabilization of Reactive Species by Supramolecular Encapsulation. *Chem. Soc. Rev.* **2016**, *45*, 1720-1737.

(9) (a) Hooley, R. J.; Rebek Jr, J., Chemistry and Catalysis in Functional Cavitands. *Chem. Biol.* **2009**, *16*, 255-264. (b) Pinacho Crisóstomo, F. R.; Lledó, A.; Shenoy, S. R.; Iwasawa, T.; Rebek, J., Recognition and Organocatalysis with a Synthetic Cavitand Receptor. *J. Am. Chem. Soc.* **2009**, *131*, 7402-7410.

(10) (a) Zelder, F. H.; Rebek Jr, J., Cavitand Templated Catalysis of Acetylcholine. *Chem. Commun.* **2006**, 753-754. (b) Richeter, S.; Rebek, J., Catalysis by a Synthetic Receptor Sealed at One End and Functionalized at the Other. *J. Am. Chem. Soc.* **2004**, *126*, 16280-16281. (c) Amrhein, P.; Shivanyuk, A.; Johnson, D. W.; Rebek, J., Metal-Switching and Self-Inclusion of

Functional Cavitands. *J. Am. Chem. Soc.* **2002**, *124*, 10349-10358. (d) Starnes, S. D.; Rudkevich, D. M.; Rebek, J., Cavitand–Porphyrins. *J. Am. Chem. Soc.* **2001**, *123*, 4659-4669. (e) Starnes, S. D.; Rudkevich, D. M.; Rebek, J., A Cavitand–Porphyrin Hybrid. *Org. Lett.* **2000**, *2*, 1995-1998. (f) Gibson, C.; Rebek, J., Recognition and Catalysis in Allylic Alkylations. *Org. Lett.* **2002**, *4*, 1887-1890.

(11) For a review on cavitand-appended metal catalysts see: Iwasawa, T., Recent Developments of Cavitand-Recessed Type Metal Catalysts. *Tetrahedron. Lett.* **2017**, *58*, 4217-4226.

(12) Degardin, M.; Busseron, E.; Kim, D.-A.; Ajami, D.; Rebek, J., Deep Cavitands Featuring Functional Acetal-Based Walls. *Chem. Commun.* **2012**, *48*, 11850-11852.

(13) (a) Mettry, M.; Moehlig, M. P.; Gill, A. D.; Hooley, R. J., Alkane Oxidation Catalysed by a Self-Folded Multi-Iron Complex. *Supramol. Chem.* **2017**, *29*, 120-128. (b) Hong, J.; Djernes, K. E.; Lee, I.; Hooley, R. J.; Zaera, F., Heterogeneous Catalyst for the Selective Oxidation of Unactivated Hydrocarbons Based on a Tethered Metal-Coordinated Cavitand. *ACS Catal.* **2013**, *3*, 2154-2157.

(14) (a) Purse, B. W.; Ballester, P.; Rebek, J., Reactivity and Molecular Recognition: Amine Methylation by an Introverted Ester. *J. Am. Chem. Soc.* **2003**, *125*, 14682-14683. (b) Amrhein, P.; Shivanyuk, A.; Johnson, D. W.; Rebek, J., Metal-Switching and Self-Inclusion of Functional Cavitands. *J. Am. Chem. Soc.* **2002**, *124*, 10349-10358.

(15) Kanaura, M.; Ito, K.; Schramm, M. P.; Ajami, D.; Iwasawa, T., Cavitands with inwardly and outwardly directed functional groups. *Tetrahedron Lett.* **2015**, *56*, 4824-4828.

(16) Soler, M.; Figueras, E.; Serrano-Plana, J.; González-Bártulos, M.; Massaguer, A.; Company, A.; Martínez, M. Á.; Malina, J.; Brabec, V.; Feliu, L.; Planas, M.; Ribas, X.; Costas, M., Design, Preparation, and Characterization of Zn and Cu Metallopeptides Based On Tetradentate Aminopyridine Ligands Showing Enhanced DNA Cleavage Activity. *Inorg. Chem.* **2015**, *54*, 10542-10558.

(17) Cussó, O.; Garcia-Bosch, I.; Ribas, X.; Lloret-Fillol, J.; Costas, M., Asymmetric Epoxidation with H₂O₂ by Manipulating the Electronic Properties of Non-heme Iron Catalysts. *J. Am. Chem. Soc.* **2013**, *135*, 14871-14878.

(18) Moran, J. R.; Ericson, J. L.; Dalcanale, E.; Bryant, J. A.; Knobler, C. B.; Cram, D. J., Vases and kites as cavitands. *J. Am. Chem. Soc.* **1991**, *113*, 5707-5714.

(19) Hooley, R. J.; Shenoy, S. R.; Rebek, J., Electronic and Steric Effects in Binding of Deep Cavitands. *Org. Lett.* **2008**, *10*, 5397-5400.

(20) For some binding experiments the NMR spectra were taken at 240 K to obtain sharper peaks and facilitate assignment. Similar signals can be observed at 298 K albeit slightly broader, due to guest tumbling at rates closer to the NMR time scale.

(21) Ajami, D.; Iwasawa, T.; Rebek, J., Experimental and Computational Probes of the Space in a Self-Assembled Capsule. *Proc. Natnl. Acad. Sci.* **2006**, *103*, 8934-8936.

(22) (a) Lledo, A.; Rebek Jr, J., Self-Folding Cavitands: Structural Characterization of the Induced-Fit Model. *Chem. Commun.* **2010**, *46*, 1637-1639. (b) Lledo, A.; Rebek Jr, J., Deep Cavitand Receptors with pH-Independent Water Solubility. *Chem. Commun.* **2010**, *46*, 8630-8632.

(23) For a thorough study of the cavity effect on a reminiscent catalytic process see: Kanaura, M.; Endo, N.; Schramm, M. P.; Iwasawa, T., Evaluation of the Reactivity of Metallocatalytic Cavities in the Dimerization of Terminal Alkynes. *Eur. J. Org. Chem.* **2016**, *2016*, 4970-4975.

(24) Krebs, C.; Galonić Fujimori, D.; Walsh, C. T.; Bollinger, J. M., Non-Heme Fe(IV)–Oxo Intermediates. *Acc. Chem. Res.* **2007**, *40*, 484-492.

(25) Sahu, S.; Goldberg, D. P., Activation of Dioxygen by Iron and Manganese Complexes: A Heme and Nonheme Perspective. *J. Am. Chem. Soc.* **2016**, *138*, 11410-11428. b) Puri, M.; Que, L., Toward the Synthesis of More Reactive $S = 2$ Non-Heme Oxoiron(IV) Complexes. *Acc. Chem. Res.* **2015**, *48*, 2443-2452. c) Nam, W., Synthetic Mononuclear Nonheme Iron–Oxygen Intermediates. *Acc. Chem. Res.* **2015**, *48*, 2415-2423. d) Ray, K.; Pfaff, F. F.; Wang, B.; Nam, W., Status of Reactive Non-Heme Metal–Oxygen Intermediates in Chemical and Enzymatic Reactions. *J. Am. Chem. Soc.* **2014**, *136*, 13942-13958.

(26) McDonald, A. R.; Que, L., High-Valent Nonheme Iron-Oxo Complexes: Synthesis, Structure, and Spectroscopy. *Coord. Chem. Rev.* **2013**, *257*, 414-428.

(27) As with other neutral substrates, we did not find any evidence to support the formation of a kinetically stable host-guest complex with thioanisole.

(28) A recent report describes an iron complex fused to a calixarene from which a highly unstable $\text{Fe}^{\text{IV}}(\text{O})$ is obtained, see: Ségaud, N.; De Thomasson, C.; Daverat, C.; Sénéchal-David, K.; Dos Santos, A.; Steinmetz, V.; Maître, P.; Rebilly, J.-N.; Banse, F.; Reinaud, O., Mimicking the Regulation Step of Fe-Monooxygenases: Allosteric Modulation of FeIV-Oxo Formation by Guest Binding in a Dinuclear ZnII–FeII Calix[6]arene-Based Funnel Complex. *Chem. Eur. J.* **2017**, *23*, 2894-2906.

TOC Artwork

